Combustion and Flame 160 (2013) 1636–1649

Contents lists available at SciVerse ScienceDirect

Combustion and Flame

journal homepage: www.elsevier.com/locate/combustflame

Numerical study of CO and CO_2 formation in CH_4/H_2 blended flame under MILD condition

Amir Mardani [a,*], Sadegh Tabejamaat [b], Shahla Hassanpour [b]

[a] Department of Aerospace Engineering, Sharif University of Technology, Azadi Str., P.O. Box 11365-11155, Tehran, Iran
[b] Department of Aerospace Engineering, Amirkabir University of Technology, Hafez Str., Tehran, Iran

ARTICLE INFO

Article history:
Received 11 June 2012
Received in revised form 29 September 2012
Accepted 7 April 2013
Available online 29 April 2013

Keywords:
Dilution
Pollutant
MILD combustion
Carbon dioxide

ABSTRACT

Reduction of air pollutants formation from hydrocarbon combustion process requires improvements in combustion systems. The moderate and intense low oxygen dilution (MILD) combustion technique is an opportunity to achieve such a goal. MILD combustion is a combustion regime which can be attained by high temperature preheating and high level dilution. In this paper, the mechanism of CO and CO_2 formation for a CH_4/H_2 fuel mixture is studied under MILD combustion condition of a jet in hot coflow (JHC) burner. This investigation is done using the computational fluid dynamics (CFD) and also zero dimensional well-stirred reactor (WSR) analysis. The RANS equations with modified k–ε equations are solved in an axisymmetric 2D computational domain. The DRM-22 reduced mechanism is considered to represent the chemical reactions. The effects of oxidizer oxygen concentration and fuel hydrogen content are studied on methane oxidation pathways. Results show that the higher hydrocarbon oxidation pathways are effective on CO and CO_2 formation under MILD condition. In the methane oxidation mechanism, the ratio between the main route and ethane route is the main reason of CO increment at higher O_2 level under MILD condition in JHC laboratory burner. The WSR analysis illustrates that a decrease of O_2 concentration in oxidizer does not necessarily lead to lower production of CO and CO_2.

1. Introduction

Greenhouse effects are results of contribution of the burning of fossil fuels. Carbon dioxide (CO_2) is one of the primary greenhouse gases which comes from combustion of carbonaceous fuels. Although carbon monoxide (CO) could contribute to greenhouse effects and is known as an air pollutant, it is usually omitted when discussing greenhouse gases as its life time is short compared to CO_2. Focusing of emission standards on regulating pollutants released by combustion processes is forcing the combustion systems toward more efficient technologies. In this framework, MILD combustion is known as a promising technique to eliminate the rate of pollutant generation in combustion systems. Higher thermal efficiency with this technique leads to lower fuel consumption which demonstrates suppression of CO_2 generation. Furthermore a more complete combustion process limits the CO contribution. MILD combustion is acronym of 'Moderate or Intense Low-oxygen Dilution' combustion. MILD combustion, HiTAC, HiCOT, and flameless combustion have been broadly known as same technologies. This combustion regime has been achieved using both high temperature preheating of reactants and high degree dilution of reaction zone, in such a way the temperature increase in the combustion process is lower than the mixture auto ignition temperature [1]. Several numerical and experimental investigations on this combustion mode have shown specific characteristics of this new combustion regime. These characteristics are briefly lower emission production and fuel consumption [2–4], higher reaction zone volume [5,6], lower combustion noise [7], more uniform temperature field, smaller oscillations of temperature in the reaction zone [7,8], sometimes colorless oxidation of fuel [7,9], lower heat release rate and lower Damköhler number in comparison with the ordinary combustion regime [8,10,11], and the influential role of molecular diffusion in the MILD combustion regime [12] .

Dally et al. [13] reported CO measurements in an experimental burner (JHC) which emulates the MILD combustion mode. CO profiles at different O_2 concentration show a reduction at lower O_2 levels. They mentioned that there is a different mechanism and chemical pathway in MILD flames in comparison with the standard atmospheric flames. Numerical modeling of the JHC burner using a RANS based code has been conducted by Christo and Dally [14], in 2005. They predicted the trends of measurements, successfully. Christo reported that the CO profile has an unexpected behavior by O_2 concentration reduction. Because higher O_2 concentration in the high preheated co-flow stream is expected to yield higher

* Corresponding author. Fax: +98 21 66022731.
E-mail addresses: Amardani@sharif.edu (A. Mardani), Sadegh@aut.ac.ir (S. Tabejamaat).

0010-2180/$ - see front matter © 2013 The Combustion Institute. Published by Elsevier Inc. All rights reserved.
http://dx.doi.org/10.1016/j.combustflame.2013.04.003

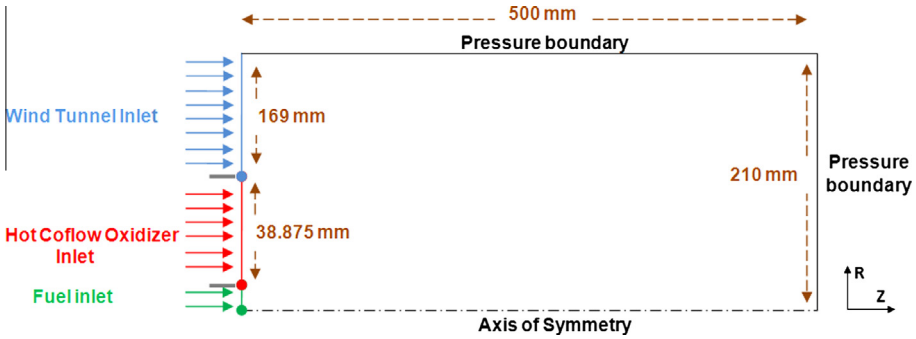

Fig. 1. Computational domain.

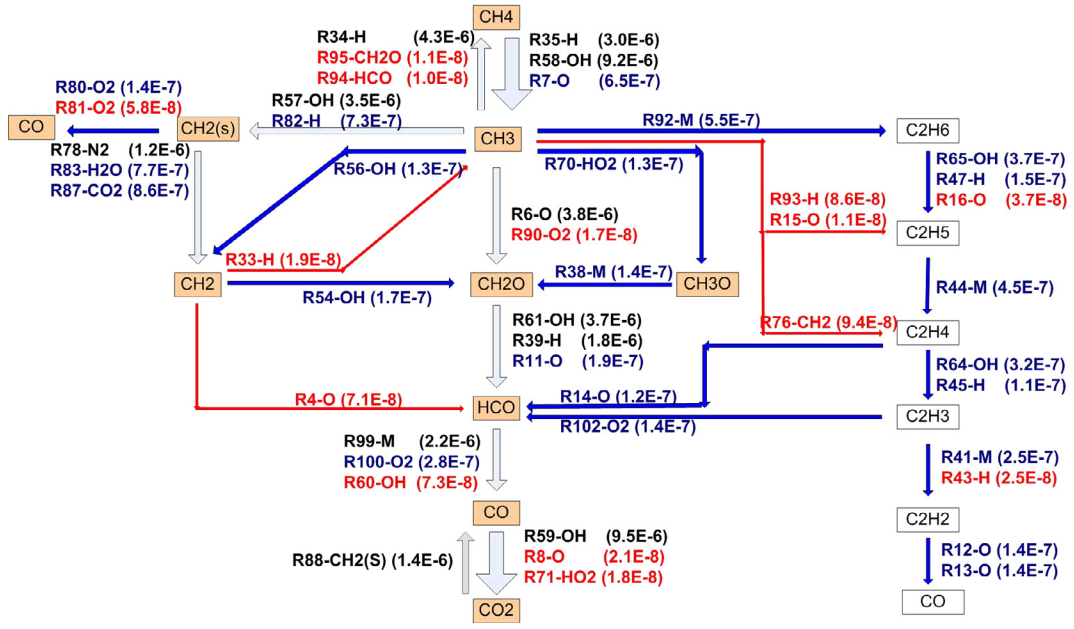

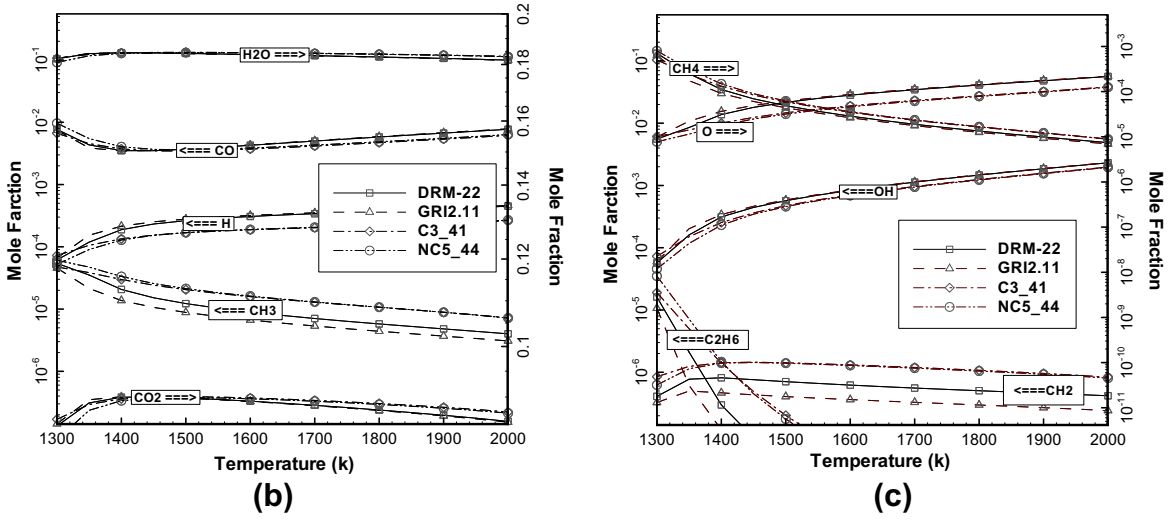

Fig. 2. (a) Methane oxidation pathways for oxidizer of 23% O_2 + 77% N_2 (by mass) in a WSR analysis (Case 1 in Table 2) at T = 1345 K and P = 1 atm for a 0.1-s residence time and stoichiometric condition. Reaction numbers refer to Table 1, while reaction rates are shown in parentheses in gmol/cm^3 s. (b and c) Comparison of predicted mole fraction of CO_2, H_2O, H, OH, O, CH_4, CH_3, CH_2 and CO for methane oxidation by oxidizer of 23% O_2 + 77% N_2 (by mass) in a WSR (Cases 2, 3 and 4 in Table 2) by four chemical mechanisms of DRM-22, GRI2.11, C3_41, and NC5_44 under conditions of P = 1 atm and a 0.1-s residence time and stoichiometric ratio.

Table 1
DRM-22 chemical mechanism.

No.	Reaction	No.	Reaction	No.	Reaction
1	$O + H + M \Leftrightarrow OH + M$	36	$H + HCO(+M) \Leftrightarrow CH_2O(+M)$	71	$HO_2 + CO \Leftrightarrow OH + CO_2$
2	$O + H_2 \Leftrightarrow H + OH$	37	$H + HCO \Leftrightarrow H_2 + CO$	72	$HO_2 + CH_2O \Leftrightarrow HCO + H_2O_2$
3	$O + HO_2 \Leftrightarrow OH + O_2$	38	$H + CH_2O(+M) \Leftrightarrow CH_3O(+M)$	73	$CH_2 + O_2 \Leftrightarrow OH + HCO$
4	$O + CH_2 \Leftrightarrow H + HCO$	39	$H + CH_2O \Leftrightarrow HCO + H_2$	74	$CH_2 + H_2 \Leftrightarrow H + CH_3$
5	$O + CH_2(S) \Leftrightarrow H + HCO$	40	$H + CH_3O \Leftrightarrow OH + CH_3$	75	$2CH_2 \Leftrightarrow H_2 + C_2H_2$
6	$O + CH_3 \Leftrightarrow H + CH_2O$	41	$H + C_2H_2(+M) \Leftrightarrow C_2H_3(+M)$	76	$CH_2 + CH_3 \Leftrightarrow H + C_2H_4$
7	$O + CH_4 \Leftrightarrow OH + CH_3$	42	$H + C_2H_3(+M) \Leftrightarrow C_2H_4(+M)$	77	$CH_2 + CH_4 \Leftrightarrow 2CH_3$
8	$O + CO + M \Leftrightarrow CO_2 + M$	43	$H + C_2H_3 \Leftrightarrow H_2 + C_2H_2$	78	$CH_2(S) + N_2 \Leftrightarrow CH_2 + N_2$
9	$O + HCO \Leftrightarrow OH + CO$	44	$H + C_2H_4(+M) \Leftrightarrow C_2H_5(+M)$	79	$CH_2(S) + AR \Leftrightarrow CH_2 + AR$
10	$O + HCO \Leftrightarrow H + CO_2$	45	$H + C_2H_4 \Leftrightarrow C_2H_3 + H_2$	80	$CH_2(S) + O_2 \Leftrightarrow H + OH + CO$
11	$O + CH_2O \Leftrightarrow OH + HCO$	46	$H + C_2H_5(+M) \Leftrightarrow C_2H_6(+M)$	81	$CH_2(S) + O_2 \Leftrightarrow CO + H_2O$
12	$O + C_2H_2 \Leftrightarrow CH_2(S) + CO$	47	$H + C_2H_6 \Leftrightarrow C_2H_5 + H_2$	82	$CH_2(S) + H_2 \Leftrightarrow CH_3 + H$
13	$O + C_2H_2 \Leftrightarrow CO + CH_2$	48	$H_2 + CO(+M) \Leftrightarrow CH_2O(+M)$	83	$CH_2(S) + H_2O \Leftrightarrow CH_2 + H_2O$
14	$O + C_2H_4 \Leftrightarrow CH_3 + HCO$	49	$OH + H_2 \Leftrightarrow H + H_2O$	84	$CH_2(S) + CH_3 \Leftrightarrow H + C_2H_4$
15	$O + C_2H_5 \Leftrightarrow CH_3 + CH_2O$	50	$2OH(+M) \Leftrightarrow H_2O_2(+M)$	85	$CH_2(S) + CH_4 \Leftrightarrow 2CH_3$
16	$O + C_2H_6 \Leftrightarrow OH + C_2H_5$	51	$2OH \Leftrightarrow O + H_2O$	86	$CH_2(S) + CO \Leftrightarrow CH_2 + CO$
17	$O_2 + CO \Leftrightarrow O + CO_2$	52	$OH + HO_2 \Leftrightarrow O_2 + H_2O$	87	$CH_2(S) + CO_2 \Leftrightarrow CH_2 + CO_2$
18	$O_2 + CH_2O \Leftrightarrow HO_2 + HCO$	53	$OH + H_2O_2 \Leftrightarrow HO_2 + H_2O$	88	$CH_2(S) + CO_2 \Leftrightarrow CO + CH_2O$
19	$H + O_2 + M \Leftrightarrow HO_2 + M$	54	$OH + CH_2 \Leftrightarrow H + CH_2O$	89	$CH_3 + O_2 \Leftrightarrow O + CH_3O$
20	$H + 2O_2 \Leftrightarrow HO_2 + O_2$	55	$OH + CH_2(S) \Leftrightarrow H + CH_2O$	90	$CH_3 + O_2 \Leftrightarrow OH + CH_2O$
21	$H + O_2 + H_2O \Leftrightarrow HO_2 + H_2O$	56	$OH + CH_3 \Leftrightarrow CH_2 + H_2O$	91	$CH_3 + H_2O_2 \Leftrightarrow HO_2 + CH_4$
22	$H + O_2 + N_2 \Leftrightarrow HO_2 + N_2$	57	$OH + CH_3 \Leftrightarrow CH_2(S) + H_2O$	92	$2CH_3(+M) \Leftrightarrow C_2H_6(+M)$
23	$H + O_2 + AR \Leftrightarrow HO_2 + AR$	58	$OH + CH_4 \Leftrightarrow CH_3 + H_2O$	93	$2CH_3 \Leftrightarrow H + C_2H_5$
24	$H + O_2 \Leftrightarrow O + OH$	59	$OH + CO \Leftrightarrow H + CO_2$	94	$CH_3 + HCO \Leftrightarrow CH_4 + CO$
25	$2H + M \Leftrightarrow H_2 + M$	60	$OH + HCO \Leftrightarrow H_2O + CO$	95	$CH_3 + CH_2O \Leftrightarrow HCO + CH_4$
26	$2H + H_2 \Leftrightarrow 2H_2$	61	$OH + CH_2O \Leftrightarrow HCO + H_2O$	96	$CH_3 + C_2H_4 \Leftrightarrow C_2H_3 + CH_4$
27	$2H + H_2O \Leftrightarrow H_2 + H_2O$	62	$OH + C_2H_2 \Leftrightarrow CH_3 + CO$	97	$CH_3 + C_2H_6 \Leftrightarrow C_2H_5 + CH_4$
28	$2H + CO_2 \Leftrightarrow H_2 + CO_2$	63	$OH + C_2H_3 \Leftrightarrow H_2O + C_2H_2$	98	$HCO + H_2O \Leftrightarrow H + CO + H_2O$
29	$H + OH + M \Leftrightarrow H_2O + M$	64	$OH + C_2H_4 \Leftrightarrow C_2H_3 + H_2O$	99	$HCO + M \Leftrightarrow H + CO + M$
30	$H + HO_2 \Leftrightarrow O_2 + H_2$	65	$OH + C_2H_6 \Leftrightarrow C_2H_5 + H_2O$	100	$HCO + O_2 \Leftrightarrow HO_2 + CO$
31	$H + HO_2 \Leftrightarrow 2OH$	66	$2HO_2 \Leftrightarrow O_2 + H_2O_2$	101	$CH_3O + O_2 \Leftrightarrow HO_2 + CH_2O$
32	$H + H_2O_2 \Leftrightarrow HO_2 + H_2$	67	$2HO_2 \Leftrightarrow O_2 + H_2O_2$	102	$C_2H_3 + O_2 \Leftrightarrow HCO + CH_2O$
33	$H + CH_2(+M) \Leftrightarrow CH_3(+M)$	68	$HO_2 + CH_2 \Leftrightarrow OH + CH_2O$	103	$C_2H_4(+M) \Leftrightarrow H_2 + C_2H_2(+M)$
34	$H + CH_3(+M) \Leftrightarrow CH_4(+M)$	69	$HO_2 + CH_3 \Leftrightarrow O_2 + CH_4$	104	$C_2H_5 + O_2 \Leftrightarrow HO_2 + C_2H_4$
35	$H + CH_4 \Leftrightarrow CH_3 + H_2$	70	$HO_2 + CH_3 \Leftrightarrow OH + CH_3O$		

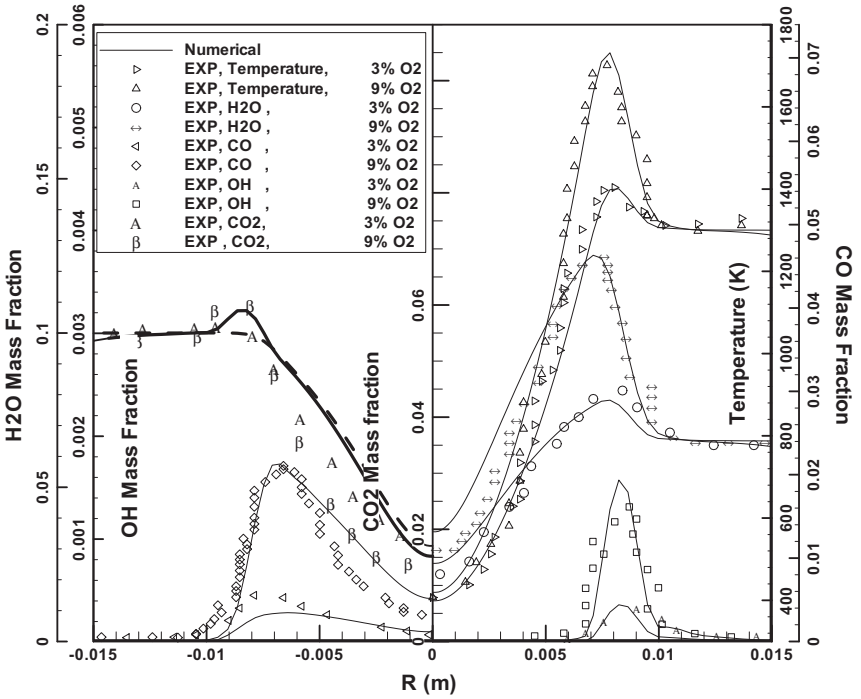

Fig. 3. Comparison of radial profiles of numerical prediction and experimental measurements for two oxidizer concentrations of 3% and 9% O_2 at Z = 30 mm (Cases 5 and 6 in Table 2).

conversion of CO to CO_2. They reported such an observation under laminar MILD flame and guessed that the pathway of CO conversion to CO_2 could change under MILD condition. de Joannon et al. [15], using a well-stirred reactor (WSR) configuration, reported

Table 2
Numerical experiments.

No.	Fuel	Hot oxidizer composition	CFD	WSR	Chemical mechanism	Conditions of WSR (P^1,R^2,T^3,E^4)
1	100% CH_4	23% O_2 + 77% N_2		*	DRM-22	(1,0.1,1345,1)
2	100% CH_4	23% O_2 + 77% N_2		*	GRI2.11	(1,0.1,1345,1)
3	100% CH_4	23% O_2 + 77% N_2		*	C3-41	(1,0.1,1345,1)
4	100% CH_4	23% O_2 + 77% N_2		*	NC5-44	(1,0.1,1345,1)
5	20% H_2 + 80% CH_4	9% O_2 + 6.5% H_2O + 5.5% CO_2 + 79% N_2	*		DRM-22	–
6	20% H_2 + 80% CH_4	3% O_2 + 6.5% H_2O + 5.5% CO_2 + 85% N_2	*		DRM-22	–
7	100% CH_4	9% O_2 + 91% N_2		*	DRM-22	(1,0.1,1345,1)
8	100% CH_4	3% O_2 + 97% N_2		*	DRM-22	(1,0.1,1345,1)
9	20% H_2 + 80% CH_4	9% O_2 + 6.5% H_2O + 5.5% CO_2 + 79% N_2		*	DRM-22	(1,0.1,1345,1)
10	20% H_2 + 80% CH_4	3% O_2 + 6.5% H_2O + 5.5% CO_2 + 85% N_2		*	DRM-22	(1,0.1,1345,1)
11	20% H_2 + 80% CH_4	9% O_2 + 91% N_2		*	DRM-22	(1,0.1,1345,0.8–1.2)
12	100% CH_4	[3–23]% O_2 + [97–77]% N_2		*	DRM-22	(1,0.1,1345,1)
13	20% H_2 + 80% CH_4	[3–23]% O_2 + [97–77]% N_2		*	DRM-22	(1,0.1,1345,1)
14	100% CH_4	100% O_2		*	DRM-22	(1,0.1,1200–2200,1)
15	20% H_2 + 80% CH_4	100% O_2		*	DRM-22	(1,0.1,1200–2200,1)
16	100% CH_4	3% O_2 + 97%		*	DRM-22	(1,0.1,1200–2200,1)
17	20% H_2 + 80% CH_4	3% O_2 + 97%		*	DRM-22	(1,0.1,1200–2200,1)
18	20% H_2 + 80% CH_4	23% O_2 + 77% N_2		*	DRM-22	(1,0.01–0.28,1345,1)
19	20% H_2 + 80% CH_4	9% O_2 + 91% N_2		*	DRM-22	(1,0.01–0.28,1345,1)
20	20% H_2 + 80% CH_4	3% O_2 + 97% N_2		*	DRM-22	(1,0.01–0.28,1345,1)

1: Pressure in atm; 2: Residence time in sec; 3: Temperature in Kelvin; 4: Equivalence Ratio.

that the oxidation and pyrolitic regimes are the working conditions for diluted combustion. The former is suitable for reburning technology which results in CO and H_2O as main reaction products. The latter could be considered for a reasonable explanation of flameless combustion, which leads to large production of CO and H_2. Extremely reduction of NOx, CO, and UHC emissions under flameless condition is also reported by Li et al. [16], in a multiple jets premixed gas turbine combustor and a swirling jet combustor. Recirculation in MILD combustion includes CO_2 and steam in reaction zone. Glarborg and Bentzen [17] and Sabia et al. [18] showed that carbon dioxide and steam can modify the chemical pathways involved in oxidation processes. Chinnici et al. [19] reported the presence of temperature oscillations in the MILD combustion system due to carbon dioxide in the reaction zone. de Joannon et al. [20], in a Jet Stirred Flow Reactor, investigated the temperature oscillation in methane MILD combustion experimentally and numerically. They reported that the competition between oxidation and recombination channels is stressed under the high dilution and preheated condition. This competition is responsible for temperature oscillation modulation in stoichiometric and lean conditions. Dally et al. [21] extended the applicability of MILD combustion to solid biomass fuel combustion in a laboratory burner. Their measurement of combustion chamber exhaust gas emissions showed the reduction of NOx emission and increment of CO by transition from conventional to MILD combustion using natural gas. A MILD combustion burner fed with H_2 and $H_2/CO_2/H_2O$ mixtures studied by Shabanian et al. [22] both numerically and experimentally. They reported the values of NOx and CO within the exhaust.

Methane oxidation to CO and CO_2 under high and low temperature has been studied in different Refs. [23,24], but CO and CO_2 formation under MILD condition could be still studied in more details. Indeed this study is in continuation of our previous reports on MILD combustion [12,25,26], and its main objective is to illustrate the effect of oxygen concentration on methane oxidation to CO and CO_2 under MILD combustion regime. Although the JHC burner configuration has shown its strength to emulate MILD combustion under controlled condition and has already been used in some studies [27–30] to investigate the MILD combustion characteristics, it has been less mentioned regarding the main objective of present work. In this framework, a CFD analysis of JHC burner using the RANS equations is accompanied by zero dimensional analysis of a WSR to explore the carbon monoxide and carbon dioxide formation under MILD condition for different oxidizer O_2 levels and two fuels of methane and methane-hydrogen mixture.

2. Numerical method

In CFD part, the JHC burner is used for modeling. The numerical method is the same as the method used in the authors' previous reports [12,25,26]. The JHC burner is a co-flow burner which is mounted in a wind tunnel in which fuel jet issues into a co-flow preheated and diluted air. Fuel is mixture of 20% H_2 and 80% CH_4 in mass basis. The fuel jet Reynolds number is around 10,000 and the velocity of hot co-flow air is 3.2 m/s. The temperature of fuel, hot co-flow and wind tunnel air are 305, 1300, and 305 K, respectively. Modeling is performed using the 2D-axisyymetric RANS equations and modified k–ε equations. The $c_{\varepsilon 1}$ coefficient in eddy dissipation equation is changed from 1.44 to 1.6, according to the results of Christo and Dally [14], in order to improve the standard k–ε model. Velocity profiles at the inlets are estimated from non-reacting flow field modeling inside the burner. According to the results of previous reports [12,14,25,31], modeling of JHC burner is less sensitive to the turbulence intensity at hot co-flow and wind tunnel inlets, although the turbulence intensity at the fuel inlet is important and is set to 7%. Patankar SIMPLER algorithm, with a third order Quick discretization method, are used to solve the equations [32]. Using the first Fick's law and the binary diffusion coefficients, found from molecular kinetic theory [33], differential diffusion method is considered but the radiation effect is neglected. Insignificant effect of radiation on JHC flame modeling has been reported by Christo and Dally in 2005 [14]. The turbulence and chemistry interaction is modeled by EDC model. The EDC model [34], which is an extension of the eddy-dissipation model (ED) to include detailed chemical mechanisms in turbulent flows, uses finite rate model in conjunction with the flow field turbulence characteristics. The model assumes that reaction take places in the small turbulent structures, namely the fine scales. The volume fraction of the fine scales is modeled using flow field turbulence characteristics, in which each structure is a Constant-Pressure-Reactor (CPR) and homogeneous. Species are assumed

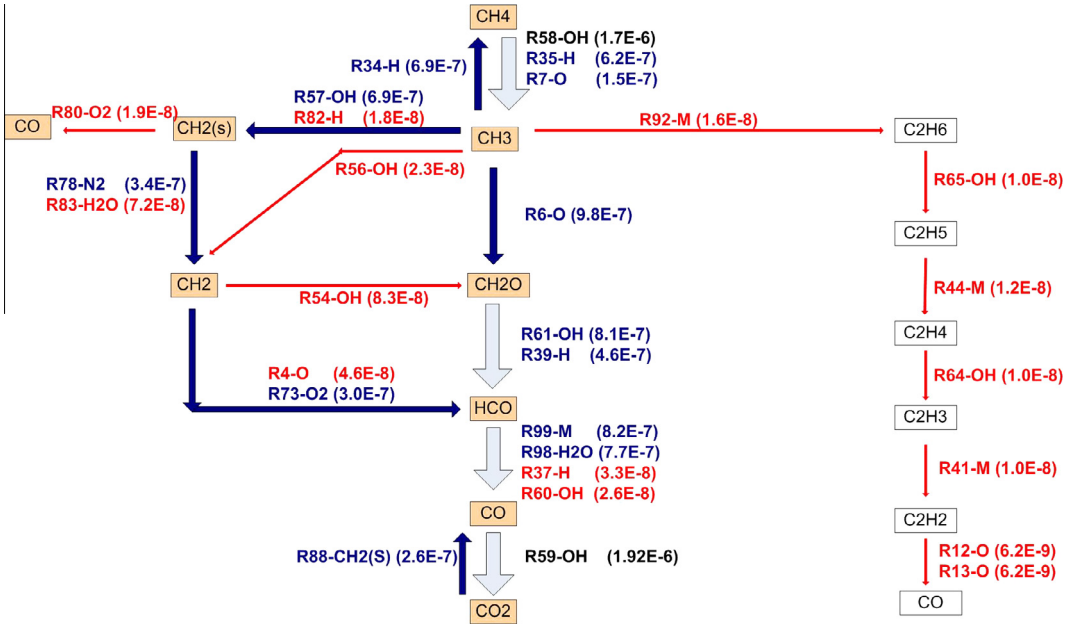

Fig. 4. Methane oxidation pathways for oxidizers of 9% O_2 + 91% N_2 (by mass) in a WSR analysis (Cases 7 in Table 2) at T = 1345 K and P = 1 atm for a 0.1-s residence time and stoichiometric condition. Reaction numbers refer to Table 1, while reaction rates are shown in parentheses in gmol/cm^3 s.

to react in the fine structures over a time scale according to Arrhenius finite rate law and detailed chemical mechanisms. This model is used extensively in MILD combustion modeling [14,30,35]. Moreover, its performance under this new combustion regime has been studied in detail by De et al. [36]. Dally's burner equivalent CFD computational domain is shown in Fig. 1.

Characteristics of the MILD combustion regime such as low reaction rates and comparable reaction and turbulence time scales [8,11] seem to let us suppose the reaction zone composition as a outlet of Well-stirred Reactor (WSR) [37]. The characteristic of the WSR entails the high level mixing (i.e. the more homogeneous mixture) and also a long average residence time inside the reactor (i.e. finite rate reactions). Linking between MILD combustion and a WSR characteristics has been separately reported by Plessing et al. [10] and also Weber et al. [38]. Attempt of De Joannon et al. [15] for schematization of flameless combustion regime has been made using a WSR configuration. They concluded that the fairly similarity between concepts of MILD and WSR are more related to oxidation in reburning technology in terms of temperature and composition. On the other hand fine structures, in the EDC model, are assumed as isobaric, adiabatic and perfectly stirred reactors. From this point of view, it is possible to find some similarities between characteristics of the EDC model and the WSR qualitatively. Therefore the WSR analysis could be a useful opportunity to be a preliminary analysis to catch a glimpse of methane oxidation process under low oxygen and preheated conditions before studying the main features of MILD regime by reacting flow analysis, here. The WSR analysis is performed by solving the species conservations equations under constant reactor temperature over a residence time using an in-house Fortran code which includes some subroutines of the CHEMKIN open source code [39].

3. Chemical mechanism

To study CO and CO_2 formation, following the reaction pathways of methane oxidation could be a helpful and useful approach. For such an approach, choosing an appropriate and accurate chemical mechanism is necessary at the first of present work. To this end, there have been many detailed chemical mechanisms developed to describe methane oxidation. They consist of a large number of species and reactions which using them in reacting flow modeling entails a high computational cost. Due to considerations of our computational facilities, choosing a costly appropriate chemical mechanism, which to be reasonably able to describe the main features of methane oxidation under MILD condition, is absolutely vital in the present work. Previous reports of the author and the other different reports [25,26,40], showed an acceptable accuracy of reduced chemical mechanism of DRM-22 [41] in comparison with the full chemical mechanism of GRI2.11.

The DRM-19 and DRM-22 [41] are reduced versions of the GRI1.2 [42], which their performance in capturing some features of MILD combustion has been identified before. Parente et al. [40] reported that there is a good agreement between the results of the DRM-19 and the GRI3.0 [43] for the modeling of MILD combustion. On the other hand, under MILD condition, in addition to the uniformity of temperature field, extinction and re-ignition occur broadly in the reaction zone as a result of low oxygen concentration and high temperature preheating. Therefore, a selected chemical mechanism should be able to capture such as phenomena. According to the report by Kazakov and Frenklach [41], the DRM-22 shows a better performance than DRM-19 in predicting ignition delay time and laminar flame speed in atmospheric pressure. Therefore it seems that DRM-22 could be a good candidate for representing the chemical mechanism in the MILD combustion modeling. In this way, considering some more detailed analysis could be beneficial to increase confidence in the reasonable accuracy of DRM-22 in the prediction of methane oxidation pathways especially relating to minor species, for the purposes of present work here. The latter concern has been investigated by some more detailed analysis as follows.

Methane, which exhibits some unique combustion characteristics like high ignition temperature and low flame speed, is widely researched into the comprehensive chemical mechanism [23]. Moreover much effort has been directed to attain simplified mechanisms from larger comprehensive mechanisms for different combustion modes. At first, as the main aim of the present work, an attempt has been made to choose a suitable chemical mechanism

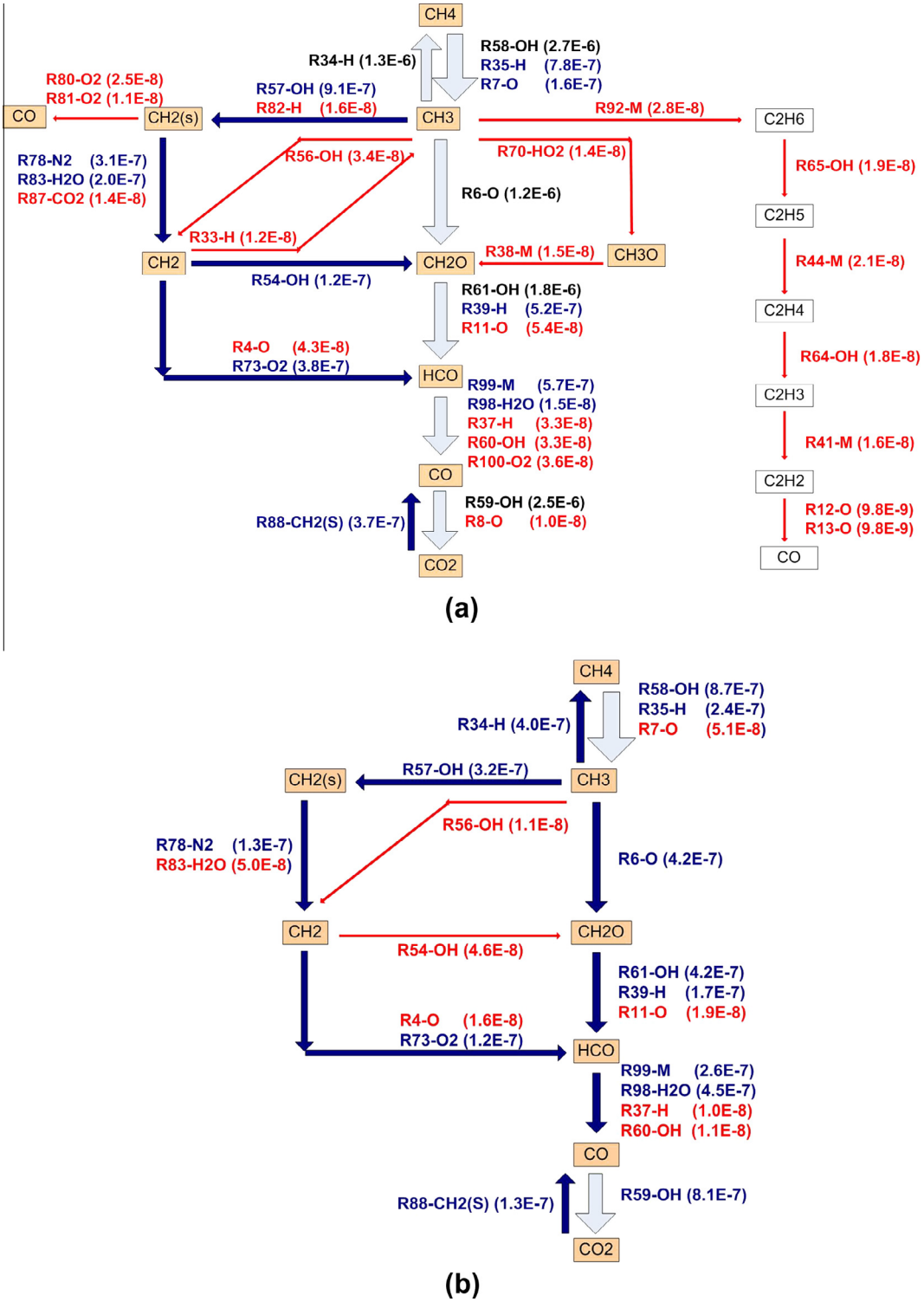

Fig. 5. Oxidation pathways of 80% CH_4 + 20% H_2 (by mass) for two oxidizers of (a) 9% O_2 + 5.5% CO_2 + 6.5% H_2O + 79% N_2, (b) 3% O_2 + 5.5% CO_2 + 6.5% H_2O + 85% N_2 (by mass) in a WSR analysis (Cases 9 and 10 in Table 2) at T = 1345 K and P = 1 atm for a 0.1-s residence time and stoichiometric condition. Reaction numbers refer to Table 1, while reaction rates are shown in parentheses in gmol/cm^3 s.

with regard to characteristic of MILD combustion and limitation of our computational facilities. In the MILD region of JHC burner, temperature field has almost a low gradient around 1500 K and in a whole range of Low-Temperature combustion analysis of methane with air (i.e. <1500 K) which is explored by Glarborg et al. [44]. Glarborg and coworkers [23,44] illustrated the major chemical pathways in the conversion of methane to CO_2 in a well-stirred reactor at temperature of 1345 K and pressure of 1 atm for a 0.1 s residence time using the GRI2.11 chemical mechanism. Under explored condition, they reported some important features of Low-Temperature reaction pathways of methane like a strong recombination of CH_3 back to CH_4, conversion of CH_3 to CH_2O through the intermediate production of CH_3O, and producing a higher hydrocarbon than the original reactant methane (i.e. Ethane and

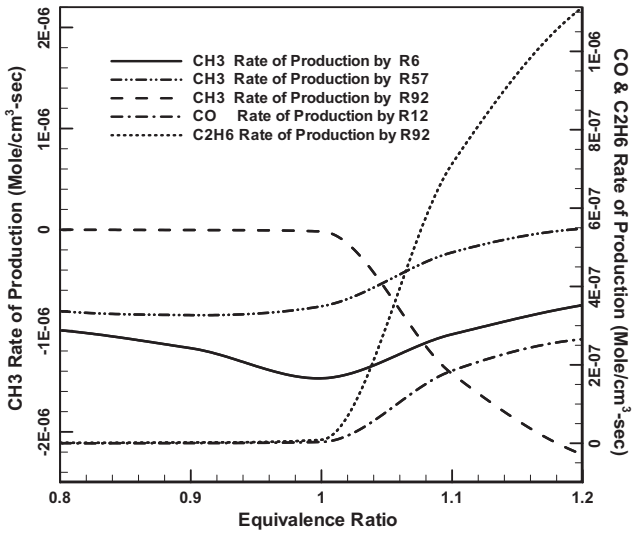

Fig. 6. Variation of CH_3, CO, and C_2H_6 rates of production by mentioned reactions in figure due to changing of equivalence ratio for WSR calculation at $T = 1345$ K, $P = 1$ atm and a residence time of 0.1 s (Case 11 in Table 2).

Acetylene). Similar to the analysis of Glarborg et al. [23,44], using the zero dimensional analysis and DRM-22 chemical mechanism, pathways of pure methane (100% CH_4) oxidation to CO and CO_2 are shown in Fig. 2a. It is for oxidizer of 23% O_2 + 77% N_2 (by mass), constant temperature of 1345 K, residence time of 0.1 s, atmospheric pressure, and stoichiometric condition. In Fig. 2a, each arrow indicates a conversion of species at its tail to the species at the head. The mentioned conversion is addressed by elementary reactions which are indicated along the length of the arrow by the numbers of reactions in the DRM-22 mechanism (Table 1) and the additional reactant species in the mentioned reaction, while the rate of destruction of reactant is quantified by the parenthetical numerical value. Furthermore the width and color of arrows gives a visual indication of the relative importance of each pathway. The elementary reactions with rates larger than 1.0e−9 (gmol/cm^3 s) are considered for pathway extractions and the other reactions are filtered. It can be concluded from Fig. 2a that the main features of methane combustion in the condition of Low-Temperature, which are mentioned above, have been captured by DRM-22 with a lower computational cost and almost same accuracy as the more complicated and comprehensive GRI2.11 mechanism.

Moreover Curran et al. [45] has mentioned the necessity of including the CH_3O_2 radical species and reactions in a reaction mechanism in order to correctly simulate the methane oxidation chemistry under high-pressure and intermediate temperature conditions. The CH_3O_2 radical species and reactions are not included in GRI-MECH family. However, the conditions of present work are not in the range of high pressure but it is in the range of intermediate temperature as mentioned above. To consider the latter point concerning the performance of DRM-22 chemical mechanism over the condition of intermediate temperature, some more studies are planned as follows. The Low-Temperature behavior of DRM-22 is studied in more detail by comparing its results with three more comprehensive detailed chemical mechanisms in Fig. 2b and c. Depicted in Fig. 2b and c are CO, CO_2, H, OH, O, CH_4, CH_3, CH_2 and H_2O predicted profiles result of the WSR analysis for fuel of methane and oxidizer of 23% O_2 + 77% N_2 (by mass) in the temperature range of 1300–2000 K, residence time of 0.1 s, atmosphere pressure, and stoichiometric condition.

These detailed chemical mechanisms are GRI2.11, C3_41, and NC5_44. C3_41 and NC5_44 are detailed chemical mechanism which are introduced by Curran et al. [46] for natural gas. C3_41 is a complete kinetic mechanism for natural gas which consists of 118 different chemical species and 663 elementary reactions. It includes three sub-mechanisms for hydrogen, methane/ethane, and C3. The hydrogen sub-mechanism is based on what was validated by O'Conaire et al. [47] in the temperature range of 298–2700 K, at pressures from 0.05 to 87 atm, and equivalence ratios from 0.2 to 6.0. The kinetic mechanism employed for the methane/ethane system is based on that published by Fischer et al. [48]. The C3 sub-mechanism is based on the work of Curran et al. [49,50].

NC5_44 is a detailed chemical mechanism for natural gas including the higher-order hydrocarbon (for example ethane (C_2H_6), propane (C_3H_8), butane (C_4H_{10}), etc.). It is developed by Curran and co-workers [51–53]. This mechanism which consists 289 species and 1580 reactions has produced quite well results for different mixtures at a wide range of pressure intervals (1–50 atm) over the temperature range 740–1550 K. It can be understood from Fig. 2b and c that the results of four chemical mechanisms are in a reasonable agreement with each other in the temperature range of 1300–2000 K, although some species like CH_2 and C_2H_6 are underpredicted using the GRI-MECH family in comparison with more complicated mechanisms of NC5_44. C3_41 and NC5_44.

In general, the DRM mechanism includes almost all key pathways through which methane oxidation is thought to occur. Therefore due to lower computational cost, DRM-22 is used as the main chemical mechanism in the present work.

4. Results

4.1. Validation

A structured grid with about 39,000 cells is selected for calculations after a grid study. CFD results have been verified by comparing with measurements of Dally et al. [13] in Fig. 3. Good agreement between numerical and experimental data for temperature and main species of H_2O and CO_2 is a good sign of reasonable accuracy of modeling of flame structure. Furthermore acceptable prediction of minor species like OH and CO could be an evidence of proper performance of intermediate reactions of chemical mechanism. Twenty numerical test cases (Table 2) are defined to conduct the research toward the main objective of the present work. They include two test cases for CFD analysis to investigate the effect of oxygen concentration on reaction zone and 18 test cases for WSR analysis to explore the effect of fuel hydrogen content, oxidizer oxygen concentration, mixture inlet temperature, and equivalence ratio on methane oxidation process to CO and CO_2 under MILD condition.

4.2. The well stirred reactor (WSR) analysis

The reasonable result of Low-Temperature analysis of methane oxidation, using DRM-22, was discussed later in Fig. 2. Importance of ethane in methane oxidation pathways under the calculated condition is the most important finding of this figure. Ethane route converts the methyl to CO through the acetylene while the main methyl oxidation route is $CH_3 \rightarrow CH_2O \rightarrow HCO \rightarrow CO \rightarrow CO_2$. These pathways were also reported by Glarborg et al. [44]. In continuation, the well-stirred reactor analysis is considered to study the combustion under MILD condition. Such an attempt provides a general overview of reaction pathways of methane oxidation under MILD condition. At first, the condition of well-stirred reactor calculation must be determined. This condition could be defined using the results of CFD modeling of JHC burner. Although the reacting

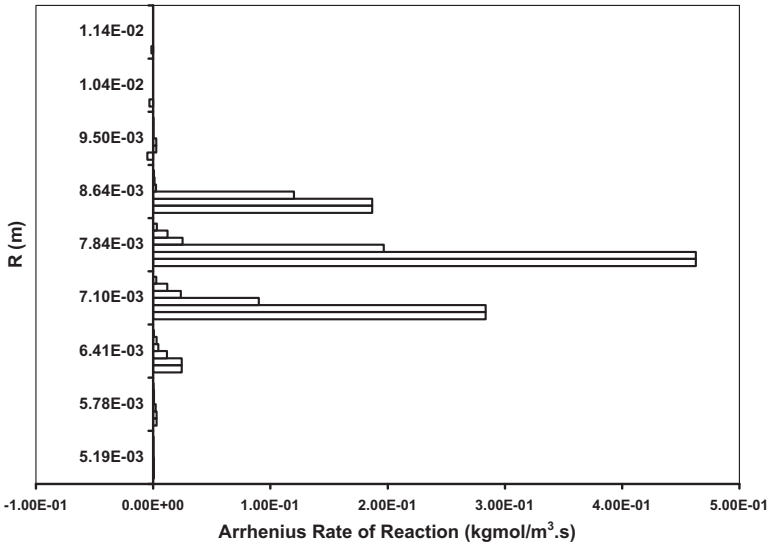

Radius(m)	Six Important Reactions →					
1.14E-02	■R-59	►R-81	■R-88	▲R-100	◄R-12	◄R-13
1.04E-02	■R-59	►R-81	◄R-12	◄R-13	■R-88	▲R-100
9.50E-03	■R-59	◄R-12	◄R-13	►R-81	■R-88	▲R-100
8.64E-03	◄R-12	◄R-13	▼R-59	▲R-98	▲R-99	●R-8
7.84E-03	◄R-12	◄R-13	▼R-59	▲R-98	▲R-99	■R-88
7.10E-03	◄R-12	◄R-13	▼R-59	▲R-98	▲R-99	■R-88
6.41E-03	◄R-12	◄R-13	▼R-59	▲R-98	▲R-99	■R-88
5.78E-03	◄R-12	◄R-13	▼R-59	▲R-98	▲R-99	▲R-100
5.19E-03	▼R-59	◄R-12	◄R-13	▲R-99	▲R-98	▲R-100
Rates change:	4.63e-1 (kg mol/m3.s)……1.39e-6(kg mol/m3.s)					
HCO → CO(▲)	Other CO consumer(►)				CO → CO2(▼)	
C2H2 → CO(◄)	Other CO producer(●)				CO2 → CO(■)	

(a)

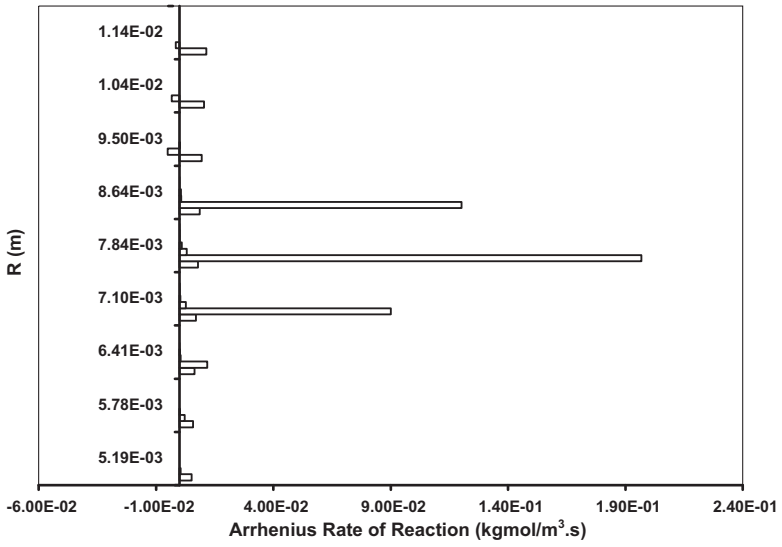

Radius(m)	Six Important Reactions →					
1.14E-02	■R-59	■R-88	◄R-87	◄R-28	▼R-8	▼R-71
1.04E-02	■R-59	■R-88	◄R-87	▼R-8	◄R-28	▼R-71
9.50E-03	■R-59	■R-88	◄R-87	▼R-8	▼R-71	▲R-10
8.64E-03	▼R-59	▼R-8	■R-88	▼R-71	◄R-87	▲R-10
7.84E-03	▼R-59	■R-88	▼R-8	▼R-71	◄R-87	▲R-10
7.10E-03	▼R-59	■R-88	▼R-8	◄R-87	▼R-71	▲R-10
6.41E-03	▼R-59	■R-88	◄R-87	▼R-71	▼R-8	▲R-10
5.78E-03	▼R-59	■R-88	▼R-71	◄R-87	▼R-8	▲R-10
5.19E-03	▼R-59	■R-88	▼R-71	◄R-87	▼R-8	▲R-10
Rates change:	1.97e-1 (kg mol/m3.s)……6.08-9(kg mol/m3.s)					
HCO → CO2(▲)	Other CO2 consumer(►)				CO → CO2(▼)	
CO2 → CO2(◄)	Other CO2 producer(●)				CO2 → CO(■)	

(b)

Fig. 7. (a) First sixth important CO containing reactions which are selected by sorting CO containing reactions according to the absolute rate of reactions and (b) First sixth important CO_2 containing reactions which are selected by sorting CO_2 containing reactions according to the absolute rate of reactions, in CFD modeling at each radial distance for $Z = 30$ mm and 9% O_2 configuration (Case 5 in Table 2).

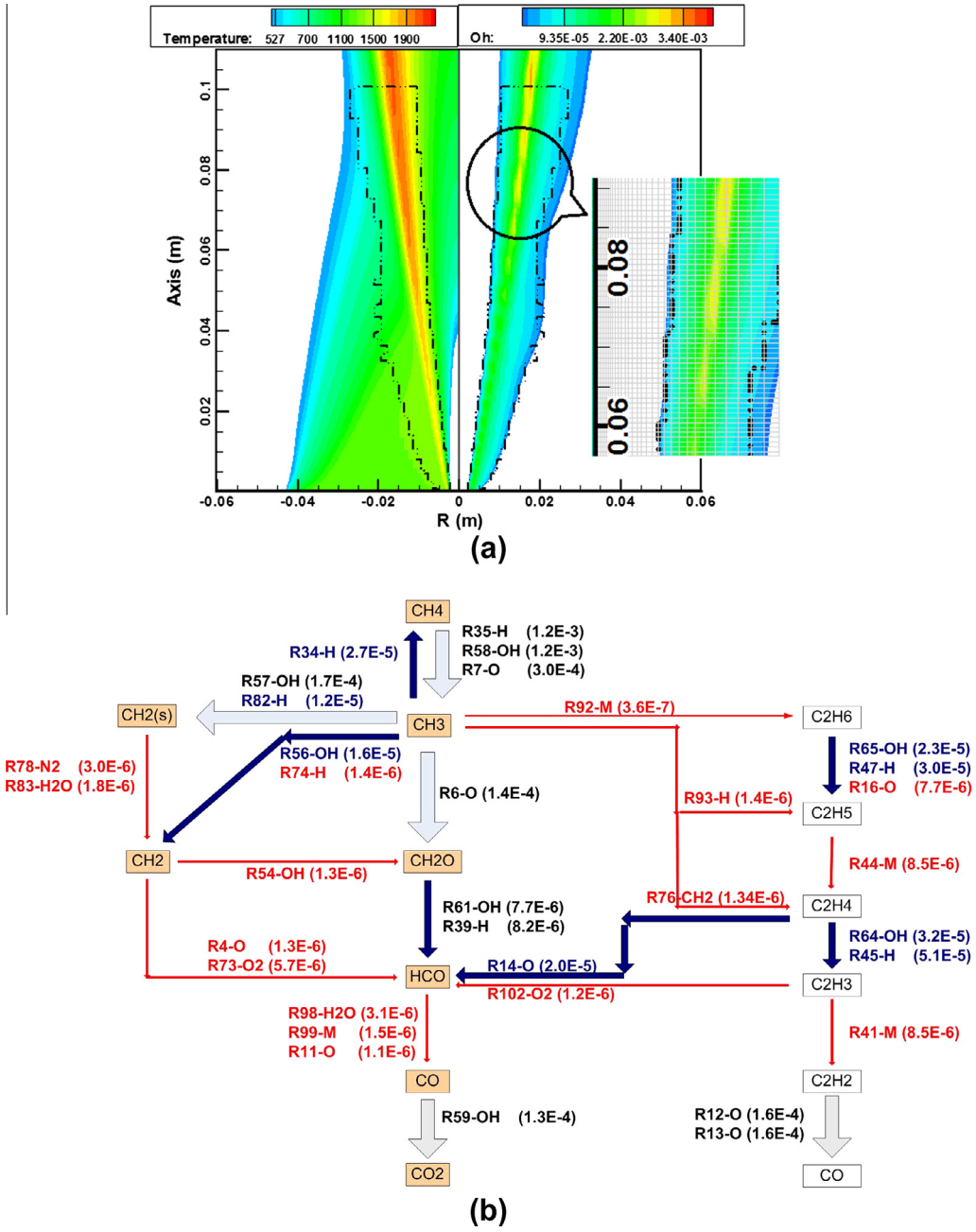

Fig. 8. Reactive flow analysis for 80% CH_4 + 20% H_2 (by mass) and oxidizers of 9% O_2 + 5.5% CO_2 + 6.5% H_2O + 79% N_2 (a) MILD region in OH and temperature contours and (b) averaged reaction pathways in the zone of part a. Reaction numbers refer to Table 1, while reaction rates are shown in parentheses in gmol/cm^3 s (Case 5 in Table 2).

flow characteristics like as residence time, temperature, and fuel/oxidizer equivalence ratio, with the exception of pressure, change locally through the MILD combustion zone (this zone is determined and discussed in Section 4.3), it has been tried to consider some appropriate values as a whole. Flow residence time using the formulation of EDC model, $\tau^* = c_\tau(\nu/\varepsilon)^{1/2}$, changes approximately between 0.02 and 1.8 s through the MILD zone. As an average, the residence time could be around 0.9 s. In the τ^* equation, ν is kinematic viscosity, ε is turbulent dissipation rate, and $c_\tau = 0.4082$ is the time scale constant. Furthermore average temperature in MILD zone is around the values $\leqslant$ 1500 K, which is in the temperature range of Low-Temperature oxidation of methane. To have a consistency between conditions of WSR calculations of all cases here and also noticing that the aim of WSR analysis in present work is more qualitative rather quantitative, WSR conditions are set to constant temperature of 1345 K, residence time of 0.1 s, atmospheric pressure, and stoichiometric condition same as the setting of Case 1 in Table 2.

MILD combustion occurs under much lower O_2 concentration than 23% O_2 (by mass). Therefore, comparing to Case 1, O_2 concentration is decreased from 23% to 9% in Fig. 4. In comparison with atmospheric condition (Fig. 2), rates of reactions are reduced but ethane still has a key role in methane oxidation. While the connecting reactions between ethane route and main CH_4 oxidation pathway (i.e. $CH_3 \rightarrow CH_2O \rightarrow HCO \rightarrow CO \rightarrow CO_2$) and also CH_3O containing reactions are weakened. On the other hand, pathway of $CH_2 \rightarrow CH_2O$ weakens although $CH_2 \rightarrow HCO$ intensifies. Another important point is that the rates of reactions R59 and R12–13 have decreased by 79% and 99%, respectively, due to reduction in inlet O_2 concentration. That means a lower relative reduction of main

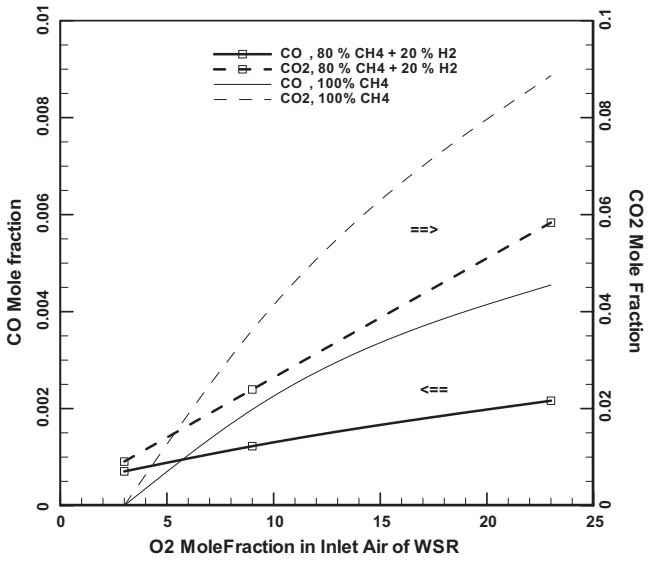

Fig. 9. Effect of oxidizer O_2 concentration on formation of CO and CO_2 for two fuels of 100% CH_4 and 80% CH_4 + 20% H_2 and oxidizer of O_2/N_2 under stoichiometric condition in a WSR at T = 1345 K and P = 1 atm for a 0.1-s residence time (Cases 12 and 13 in Table 2).

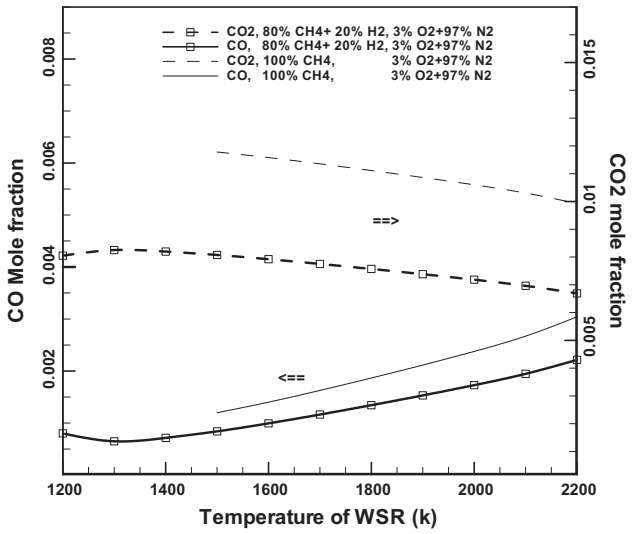

Fig. 11. Effect of WSR temperature on formation of CO and CO_2 for two fuels of 100% CH_4 and 80% CH_4 + 20% H_2 and oxidizer of 3% O_2 + 97% N_2 (by mass) under stoichiometric condition in a WSR at P = 1 atm for a 0.1-s residence time (Cases 16 and 17 in Table 2).

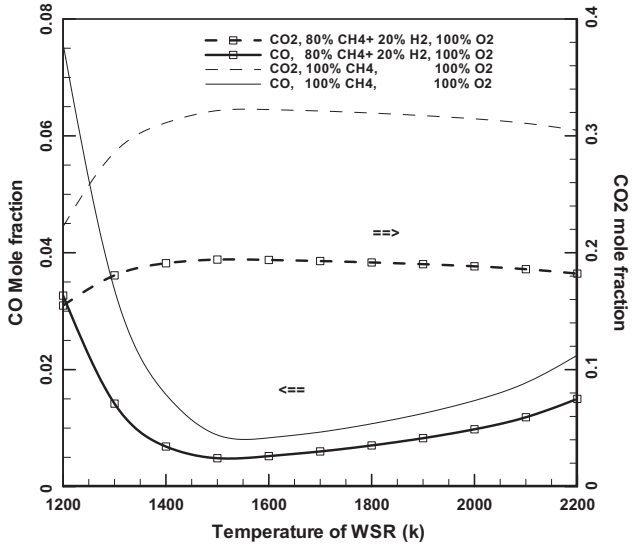

Fig. 10. Effect of WSR temperature on formation of CO and CO_2 for two fuels of 100% CH_4 and 80% CH_4 + 20% H_2 and oxidizer of 100% O_2 under stoichiometric condition in a WSR at P = 1 atm for a 0.1-s residence time (Cases 14 and 15 in Table 2).

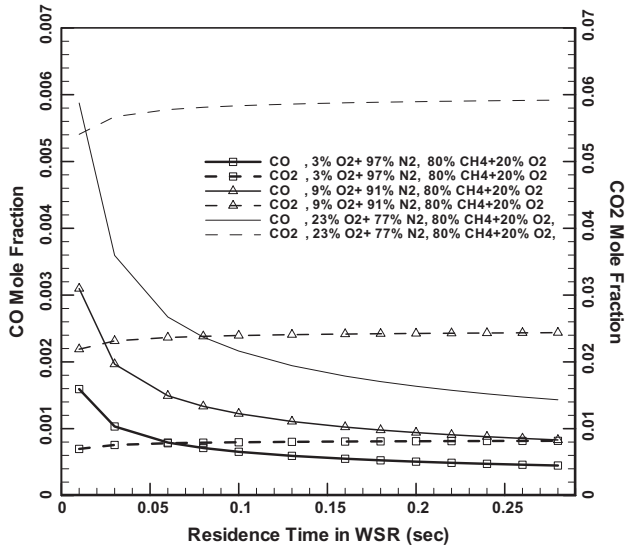

Fig. 12. Effect of residence time in WSR on formation of CO and CO_2 for fuel of 80% CH_4 + 20% H_2 and three oxidizers of 3% O_2 + 97% N_2, 9% O_2 + 91% N_2, 23% O_2 + 77% N_2 (by mass) under stoichiometric condition in a WSR at P = 1 atm (Cases 18, 19 and 20 in Table 2).

CO_2 producer reaction (i.e. R59) in respect to CO producer reactions R12 and R13.

More decreasing of O_2 concentration to 3% O_2 under the other constant conditions, reduces the reaction rates significantly to lower than 1.0e−9 (gmol/cm^3 s), therefore the reaction pathways for 3% O_2 are ignored to present here. This (i.e. the ignorable reaction rates for 3% O_2) is a good reason for adding H_2 to methane in the JHC burner fuel feeding. Because as which mentioned in Ref. [12], hydrogen addition to methane is necessary for sustaining the flame at the JHC setup for 3% O_2 and the rate of reactions become ignorable below 2% H_2 (by mass fraction). This would be discussed more as follows. In the next step, methane is enriched by 20% H_2 and methane oxidation pathways to CO and CO_2 are illustrated for 9% O_2 in Fig. 5a. It can be seen that the production of intermediate species of formaldehyde (CH_2O), which could be considered as an ignition marker, has increased as a result of intensified pathways of $CH_2 \rightarrow CH_2O$ and $CH_3 \rightarrow CH_2O$. Formation of CH_2 increases due to direct conversion of CH_3 through reaction R56 and also route of $CH_3 \rightarrow CH_2(s) \rightarrow CH_2$. Moreover an alternate route from CH_3 to CH_2O appears through the intermediate species of CH_3O. It shows that ignition process is more powerful for blended methane with H_2 in comparison with pure methane. It is in consistency with the result of Sabia et al. [54] on the higher the increase of the system reactivity with the higher fuel inlet hydrogen content. Indeed, a comparison between Figs. 4 and 5a reveals that hydrogen modifies the evolution of the methane oxidation process through the

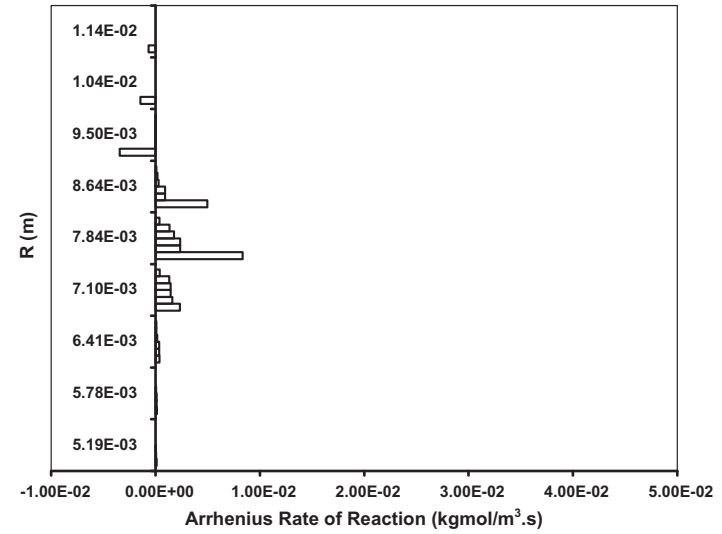

Radius(m)	Six Important Reactions →					
1.14E-02	■R-59	▲R-98	▲R-99	▲R-100	■R-88	●R-81
1.04E-02	■R-59	▲R-98	▲R-99	▲R-100	■R-88	►R-12
9.50E-03	■R-59	▲R-98	▲R-99	►R-12	►R-13	▲R-100
8.64E-03	▼R-59	►R-12	►R-13	▲R-98	▲R-99	▲R-100
7.84E-03	▼R-59	►R-12	►R-13	▲R-98	▲R-99	▲R-100
7.10E-03	▼R-59	▲R-98	►R-12	►R-13	▲R-99	▲R-100
6.41E-03	▲R-99	▲R-98	▼R-59	▲R-100	►R-12	►R-13
5.78E-03	▲R-99	▲R-100	▲R-98	▼R-59	►R-12	►R-13
5.19E-03	▲R-100	▲R-99	▲R-98	▼R-59	▲R-94	►R-12

Rates change: 8.35e-3 (kg mol/m3.s).....2.1e-7(kg mol/m3.s)

HCO → CO (▲)	Other CO consumer (◄)	CO → CO2(▼)
C2H2 → CO(►)	Other CO producer(●)	CO2 → CO (■)

(a)

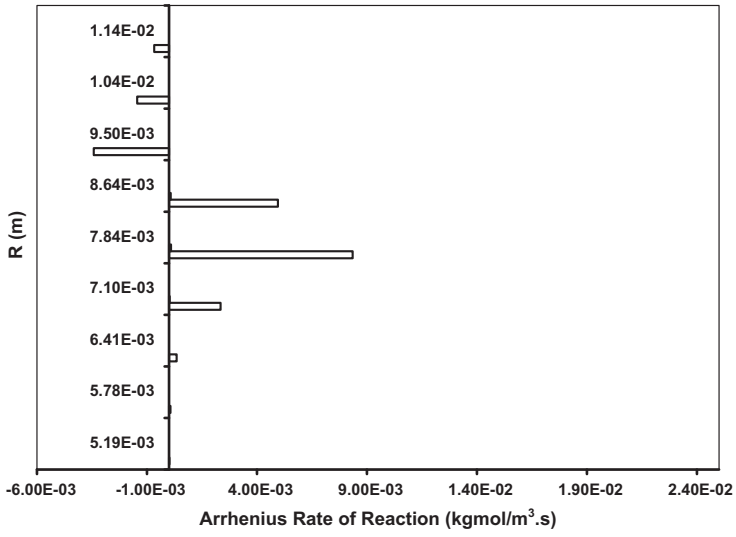

Radius(m)	Six Important Reactions →					
1.14E-02	■R-59	■R-88	◄R-87	▼R-8	◄R-28	▼R-71
1.04E-02	■R-59	■R-88	▼R-8	◄R-87	◄R-28	▼R-71
9.50E-03	■R-59	■R-88	▼R-8	◄R-87	◄R-28	▼R-71
8.64E-03	▼R-59	▼R-8	■R-88	▲R-10	▼R-71	◄R-28
7.84E-03	▼R-59	▼R-8	■R-88	▼R-71	▲R-10	◄R-87
7.10E-03	▼R-59	■R-88	▼R-8	▼R-71	▲R-10	◄R-87
6.41E-03	▼R-59	■R-88	▼R-71	▼R-8	◄R-87	▲R-10
5.78E-03	▼R-59	▼R-71	■R-88	▼R-8	◄R-87	▲R-10
5.19E-03	▼R-59	■R-88	▼R-71	◄R-87	▼R-8	▲R-10

Rates change: 8.35e-3 (kg mol/m3.s).....5.83e-9(kg mol/m3.s)

HCO → CO2(▲)	Other CO2 consumer(►)	CO → CO2(▼)
CO2 → CO2(◄)	Other CO2 producer(●)	CO2 → CO(■)

(b)

Fig. 13. (a) First sixth important CO containing reactions which are selected by sorting CO containing reactions according to the absolute rate of reactions. (b) First sixth important CO_2 containing reactions which are selected by sorting CO_2 containing reactions according to the absolute rate of reactions, in CFD modeling at each radial distance for Z = 30 mm and 3% O_2 configuration (Case 6 in Table 2).

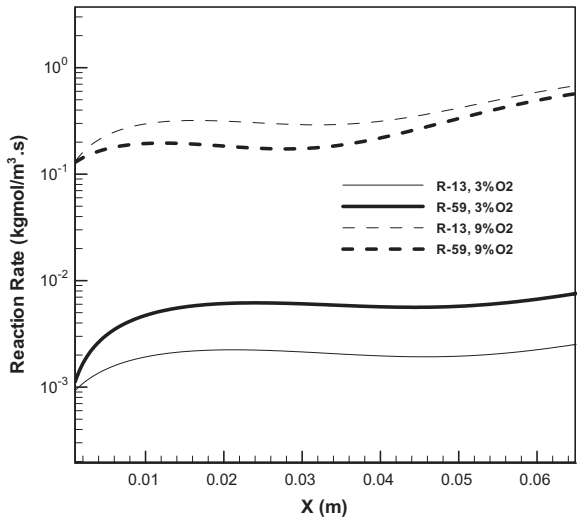

Fig. 14. Comparison of reaction rates of R13 and R59 along a line inside the reaction zone (point of maximum OH mass fraction at each distance from the fuel nozzle) inside the MILD combustion zone ($Z < 100$ mm, according to Ref. [13]) for two oxidizer of 3% and 9% (Cases 5 and 6 in Table 2).

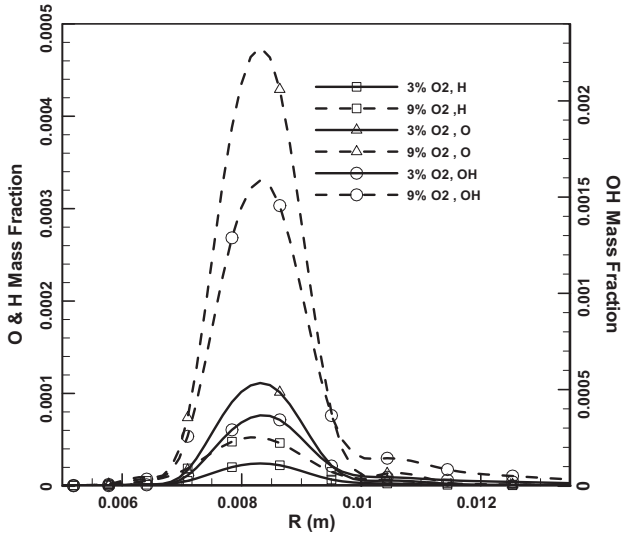

Fig. 15. Comparison of radial profiles of O, OH, and H radicals at $Z = 30$ mm for two oxidizer of 3% and 9% O_2 (Cases 5 and 6 in Table 2).

growth in reaction rates of the main methane oxidation pathways to CO_2 (i.e. $CH_3 \rightarrow CH_2O \rightarrow HCO \rightarrow CO \rightarrow CO_2$) and also a decline in reaction rates of alternative methane oxidation route to CO through the higher hydrocarbon than the original reactant methane (i.e. $CH_3 \rightarrow C_2H_6 \rightarrow C_2H_5 \rightarrow C_2H_4 \rightarrow C_2H_3 \rightarrow C_2H_2 \rightarrow CO$).

In continuation, reactions pathways for fuel of 80% CH_4 + 20% H_2 and oxidizer of 3% O_2 + 97% N_2 are shown in Fig. 5b. It can be understood from the figure that, in spite of pure methane and 3% O_2, rate of reactions are considerable as a result of presence of H_2 in the fuel mixture. Moreover, by decreasing of O_2 from 9% to 3%, rate of reactions decreases and CH_3O and ethane oxidation pathways could be ignored. Furthermore, reaction rates of all significant pathways are in the same order of magnitude. That means for 3% O_2, all shown pathways (Fig. 5b) have an approximately same importance. Weakening of pathways ended by CO and reaction R59 could be a sign of lower CO and CO_2 production at 3% O_2.

On the whole, the WSR analysis reveals that the Low-Temperature methane oxidation pathways should be thought over under diluted and preheated condition (around 1500 K). This finding, which will be noticed in the continuation of this work, is a result of WSR calculation under stoichiometric condition. On the other hand, numerical modeling of JHC burner has shown the occurrence of maximum temperature or OH mass fraction in the vicinity of stoichiometric zone and not exactly there. Therefore it would be worthwhile to investigate the effect of equivalence ratio on the CO and CO_2 formation routes to make sure about preserving overall trends in mentioned finding. In other word, it is important to know whether the higher hydrocarbon oxidation route is still important for the mixture different from stoichiometric ratio. To follow such a question, variations of C_2H_6 production from CH_3 (by R92 in the start of ethane route) and CO production from C_2H_2 (by R12 and R13 at the end of ethane route) versus inlet mixture equivalence ratio are depicted in Fig. 6 for condition of 9% O_2. Furthermore, for more detail, comparison between conversions of CH_3 to C_2H_6 (by R92), to CH_2O (by R6), and to $CH_2(s)$ (by R57) are also shown in Fig. 6 for different inlet mixture equivalence ratio. It can be understood from the figure that in the rich region (equivalence ratio higher than 1.0) the methyl conversion to C_2H_6 increases and CH_2O and $CH_2(s)$ formations decrease and also CO formation by ethane route increases. They are evidence that the higher hydrocarbon route grows in importance for rich condition. On the other hand, under lean condition, related reactions to ethane route have approximately same rates in comparison with stoichiometric condition. That means that it is possible to diversify the predicted methane oxidation pathways (to CO and CO_2) under stoichiometric condition to a little leaner condition. Indeed, stoichiometric WSR analysis could be considered as an indicator whether the higher hydrocarbon oxidation route is still important for the mixture different from stoichiometric ratio (albeit in the vicinity of stoichiometric condition) and also globally could be used to explain points regarding CO and CO_2 formation in MILD regime reaction zone even for non-stoichiometric condition.

4.3. Reacting flow analysis

In this section changes of CO and CO_2 concentration, due to variation of O_2 concentration, are studied at 30 mm from the nozzle of JHC burner. The distance of 30 mm is considered as a representative sample of MILD region because it is inside of MILD region of reaction zone ($Z < 100$ mm in JHC). In addition, Dally et al. [13] have reported experimental measurements there. In this framework, reactions of CO and CO_2 are focused.

In DRM-22, CO including reactions are R8, R10, R9, R12, R13, R17, R37, R48, R59, R60, R62, R71, R81, R86, R88, R94, R98, R99, R100 and CO_2 including reactions are R8, R10, R17, R28, R59, R71, R87, and R88. Depicted in Fig. 7a and b respectively are sorted CO and CO_2 producer and consumer reactions according to their absolute rates magnitude at each radial location of $Z = 30$ mm for 9% O_2. Moreover, the types of reactions (i.e. CO or CO_2 producer reaction) are identified in attached tables as well as their sequence. They show that in the reaction zone ($R = 7.1$–8.464 mm), the most dominant CO_2 containing reactions are R59, R88, and R8 and also the paramount important reactions including CO species are R59, R12, R13, R99, and R98. The temperature profile at $Z = 30$ mm (Fig. 3) shows that the averaged temperature in reaction zone is around 1500 K and therefore methane reaction pathways could be considered broadly similar to Fig. 5a in which the reactor inlet oxygen concentration and temperature are 9% and 1345 K, respectively. In tables of Fig. 7, symbolizing and dividing the reactions to producer and consumer of CO and CO_2 are conducted by considering methane oxidation pathways in Fig. 5a. The reaction arrangement in Fig. 7a shows that the reactions of $C_2H_2 \rightarrow CO$

(i.e. R12–13) are more important to CO formation in comparison with reactions of HCO → CO (i.e. R98–99) and $CH_2(s)$ → CO (i.e. R88). That means that in this location of JHC flame and under considered condition, ethane route attaches great importance to methane oxidation. This finding is more studied by extracting the chemical pathways in reacting flow analysis using the averaged reaction rates in MILD combustion region. MILD zone is considered as a region with Z < 100 mm and OH mass fraction of higher than one percent of maximum OH mass fraction at each axial distance from the fuel nozzle(Z). Measurements of Dally et al. [13] on JHC burner have illustrated that the mixing with fresh tunnel air affects the flame above 100 mm from the nozzle and the MILD combustion regime occurs at the region below this height. MILD zone is illustrated in Fig. 8a by dashed close line for jet Reynolds number of 10,000 and O_2 mass fraction of 9%. Reaction pathways, based on averaged rates of reactions in MILD zone (Fig. 8a), are depicted in Fig. 8b. It can be understood that the reacting flow analysis also shows the unquestionable importance of the ethane route in the methane oxidation to CO and CO_2. In other words there is a consistency between results of WSR and CFD on importance of high hydrocarbon pathways in the methane oxidation under MILD condition.

A comparison between Fig. 7a and b shows that the most important reaction for CO_2 formation (i.e. R59) has a smaller rate in comparison with reactions R12 and R13. That means that the CO producer reactions R12 and R13 have higher rates than the CO consumer reaction (or CO_2 producer reaction) R59. Moreover, the reactions R59 and R88 are significant among CO_2 containing reactions which R59 is more important than the others.

Figure 3 and both measurements of Dally et al. [13] and calculations of Christo and Dally [14] show an increment in CO and CO_2 formation by increasing of O_2 concentration. As explained in the introduction, the behavior of CO is fairly strange. To explain this phenomenon, the behavior of CO and CO_2 concentration variation due to the changes of O_2 concentration are studied in a WSR first and after that again CFD results are considered to complete the discussion about CO behavior.

Figure 9 shows the correlations between CO and CO_2 concentrations and inlet O_2 concentration in a WSR for two different fuel compositions under stoichiometric condition, residence time of 0.1 s, and temperature of 1345 K. The figure illustrates the increment in CO and CO_2 concentrations at higher O_2 levels. Furthermore, the rates of CO consumer reactions also show an increase for higher O_2 concentration (not shown here). On the other hand the WSR temperature is another important parameter which its effect on CO and CO_2 concentration is studied in Figs. 10 and 11. Depicted in Fig. 10 are the effects of combustion chamber temperature on CO and CO_2 concentration for two fuels of 100% CH_4 and 80% CH_4 + 20% H_2 and oxidizer of 100% O_2. It can be seen that the effect of temperature on CO and CO_2 concentration is different at temperature higher and lower than approximately 1500 K. That means, under condition of T < 1500 K a decrease in combustion chamber temperature increases the CO concentration and decreases CO_2 concentration, while for T > 1500 K it is quite the reverse. That is probably due to dissociation of CO_2 at temperatures higher than 1500 K. Figure 11 is the same as Fig. 10 but only for oxidizer containing 3% O_2. It shows that at lower O_2 concentration, combustion chamber temperature has an approximately identical effect on CO and CO_2 concentration and the concentration of both CO and CO_2 increase in higher combustion temperature. Therefore, the latter analysis reveals that the observed behavior (i.e. CO variation) in JHC burner, due to increase in O_2 level, could be considered approximately equivalent to the effect of flame temperature at Fig. 11. The range of temperature in the MILD zone of JHC burner passes around 1500 K with increasing oxidizer concentration.

To get a better understanding of CO and CO_2 variation by the changes in O_2 concentration, the effect of residence time on concentration of CO and CO_2 for three O_2 levels of 3%, 9%, and 21% are depicted in Fig. 12. It shows that the concentration of CO and CO_2 respectively decreases and increases with an increase of residence time. Moreover, the CO concentration is more sensitive to residence time in comparison with CO_2 for all O_2 concentrations, which this sensitivity increases for higher O_2 level. That means that fluid dynamics, which has a direct impact on residence time, is effective on CO and CO_2 production. This correlation probably grows in importance for higher O_2 levels. Therefore the residence time is responsible for some portion of CO concentration increment at higher O_2 levels in the JHC burner. It should be considered that MILD combustion and WSR have similar physical characteristics. Furthermore there is a consistency between the residence time effects at higher O_2 levels and the effect of O_2 concentration on turbulence relaminarization which is discussed extensively in the other report of the authors [26]. Damping turbulence eddies and relaminarizing of flow increases at higher O_2 concentrations because the rate of heat release increases due to increase in O_2 level.

In continuation, the variation of CO and CO_2 concentration due to the change of O_2 concentration are studied using the CFD results. In a similar approach as done for Figs. 7 and 13 is made for 3% O_2 and Z = 30 mm. This figure illustrates that the CO_2 producer and CO consumer reaction R59 has a higher rate than the CO producer reactions of the ethane route (i.e. R12 and R13), while the reverse can be understood from Fig. 7a for 9% O_2. That means the reactions R12 and R13 have higher rates than R59 for 9% O_2 and they show a contrary order for 3% O_2. So, it could be understood that the behaviors of CO and CO_2 concentrations at different O_2 levels are due to correlation between reactions R12–13 and R59. In other words, higher hydrocarbon oxidation (i.e. ethane) is responsible for CO and CO_2 concentration behavior by O_2 concentration variation. This idea is more studied by comparing reaction rats R12–13 and R59 along a line inside of the reaction zone of the jet (i.e. different Z). Such a comparison for two O_2 levels of 3% and 9% are depicted in Fig. 14. This figure shows that by changing O_2 concentration, the ratio between reaction rates of R13 and R59 changes. Furthermore, a comparison between Figs. 7a and 13a reveals that another CO producer reaction (i.e. R88) is limited at lower O_2 percent, and it might be due to lower $CH_2(s)$ production from CH_3. To understand how inlet oxygen concentration affects the methane oxidation pathways, the prominent radicals should be considered more precisely. Radical O has an important role in R12–13, which its concentration decreases at lower O_2 levels. Other important radicals like OH and H also reduce at lower O_2 concentrations (see Fig. 15). These radicals are the main reason of reactions suppression at lower oxidizer O_2 levels. Because in the first step, oxidation process starts with an attack on the CH_4 molecule by OH, O, and H radicals to produce the methyl radical and in continuation these radicals play a key role in the proceeding of both main and higher hydrocarbon oxidation pathways. In the main route, the methyl radical forms formaldehyde (CH_2O) by combining with an oxygen atom or with an OH and H radicals through the intermediate CH_2; the formaldehyde, in turn, is attacked by OH, H, and O radicals to produce the formyl radical(HCO). In the ethane route, OH attacks to C_2H_6 and C_2H_4 to form C_2H_5 and C_2H_3 respectively and the C_2H_2 combines with the oxygen atom to produce carbon monoxide (CO). As a whole, under very low oxygen concentration, in which all of the reaction rates weaken, the pathways that are unimportant at ordinary oxygen levels now could become prominent and grow in relative importance. The relevance of C2 channel in the oxidation kinetic of methane under MILD condition confirms the data reported in the results of some Refs. [15,20]. In other word importance of both Low-Temperature and High-Temperature reaction pathways in oxidation of methane under MILD condition

shows the kinetic evolution of fuels oxidation process is different in MILD regime from traditional flames.

5. Conclusion

In the present work, methane oxidation to CO and CO_2 is studied under MILD condition using a CFD modeling and also zero dimensional analysis. In the CFD approach, an experimental coflow burner is modeled using the RANS equations. The zero dimensional analysis is performed for a WSR. Results show that under MILD condition chemical pathways including conversion of methyl (CH_3) to higher hydrocarbons (i.e. ethane) are activated and some portions of methane oxides to CO through conversion to heavier ethane molecules. That means that methane Low-Temperature reaction pathways activates under MILD condition. Moreover, a decrease of O_2 concentration in oxidizer does not always leads to lower production of CO and CO_2. This can be because of dissociation of CO_2 at temperature of higher than 1500 K. Furthermore, the ratio of rates of CO producer reactions (R12 and R13: $O + C_2H_2 \Leftrightarrow CH_2(S) + CO$) in ethane oxidation route, to CO consumer reaction (R59: $OH + CO \Leftrightarrow H + CO_2$) in the main route, changes with changing of O_2 level. CFD results show that reaction rates of R12 and R13 increase and become larger than the rate of R59 for higher O_2 concentration and it reveres for lower O_2 concentration. Also, WSR analysis shows that for temperatures lower than 1500 K, an increase in temperature increases CO_2 concentration and decreases CO concentration. While the effect of temperature on CO and CO_2 concentrations reverses for temperature higher than 1500 K.

References

[1] A. Cavaliere, M.D. Joannon, Prog. Energy Combust. Sci. 30 (2004) 329–366.
[2] R. Fuse, H. Kobayashi, Y. Ju, K. Maruta, T. Niioka, Int. J. Therm. Sci. 41 (2002) 693–698.
[3] T. Hasegawa, R. Tanaka, T. Niioka, High temperature air combustion contributing to energy saving and pollutant reduction in industrial furnace, in: Proc. Int. Jt. Power Gener. Conf., ASME, Book No. G 01072, 1997, p. 259–266.
[4] H. Guo, Y.-G. Ju, K. Maruta, T. Niioka, Junichi Sato, JSME Int. J. B41 (2) (1998) 331–337.
[5] Y. Ito, A.K. Gupta, K. Yoshikawa, N. Shimo, Proc 5th High Temperature Air Combust Gasif Conf, Yokohama, Japan, 2002.
[6] 6.M. Mortberg, W. Blasiak, A.K. Gupta, J. Eng. Gas Turbines Power 129 (2007) 556.
[7] J.G. Wunning, Flameless Combustion in Thermal Process Technology, 2th Int. Semin. High Temperature Air Combust., Sweden, 2000.
[8] M. Katsuki, T. Hasegawa, Proc. Combust. Inst. 27 (1998) 3135–3146.
[9] A.K. Gupta, Flame length and ignition delay during the combustion of acetylene in high temperature air, in: Proc. 5th High Temperature Air Combust Gasifi Conf, Yokohama, Japan, 2002.
[10] T. Plessing, N. Peters, J.G. Wunning, Proc. Combust. Inst. 27 (1998) 3197–3204.
[11] H. Tsuji, A.K. Gupta, T. Hasegawa, K. Katsuki, K. Kishimoto, M. Morita, High Temperature Air Combustion: From Energy Conservation to Pollution Reduction, CRC Press, USA, 2003.
[12] A. Mardani, S. Tabejamaat, M. Ghamari, Combust. Theor. Modell. 14 (2010) 747–774.
[13] B.B. Dally, A.N. karpetis, R.S. Barlow, Combust. Inst. 29 (2002) 1147–1154.
[14] F.C. Christo, B.B. Dally, Combust. Flame 142 (2005) 117–129.
[15] M. De Joannon, A. Saponaro, A. Cavaliere, Combust. Inst. 28 (2000) 1639–1646.
[16] G. Li, E.J. Gutmark, D. Stankovic, N. Overman, M. Cornwell, L. Fuchs, V. Milosavljevic, Experimental study of flameless combustion in gas turbine combustors, in: 44th AIAA Aerospace Sciences Meeting and Exhibit AIAA, 2006, p. 546.
[17] P. Glarborg, L.L.B. Bentzen, Energy Fuel 22 (2008) 291–296.
[18] P. Sabia, M. de Joannon, A. Picarelli, A. Chinnici, R. Ragucci, Fuel 91 (2012) 238–245.
[19] A. Chinnici, M. de Joannon, P. Sabia, A. Picarelli, R. Ragucci, CO_2-driven oscillations in methane MILD combustion, in: XXXIV Meeting of the Italian Section of the Combustion Institute, doi: http://dx.doi.org/10.4405/34proci2011.II19.
[20] M. de Joannon, A. Cavaliere, T. Faravelli, E. Ranzi, P. Sabia, A. Tregrossi, Combust. Inst. 30 (2005) 2605–2612.
[21] B.B. Dally, S. Shim, R.A. Craig, P.J. Ashman, G.G. Szego, Energy Fuels 24 (2010) 3462–3470.
[22] S.R. Shabanian, M. Derudi, M. Rahimi, A. Frassoldati, A. Cuoci, T. Faravelli, Experimental and numerical analysis of syngas mild combustion, in: XXXIV Meeting of the Italian Section of the Combustion Institute, Italy.
[23] S.R. Turn, An Introduction to Combustion, Concepts and Applications, second edition, 1993.
[24] C.K. Law, Combustion Physics, Cambridge University Press, 2006.
[25] A. Mardani, S. Tabejamaat, Int. J. Hydrogen Energy 35 (2010) 11324–11331.
[26] A. Mardani, S. Tabejamaat, M. Baig Mohammadi, Combust. Theor. Modell. 15 (6) (2011) 753–772.
[27] P.R. Medwell, P.A.M. Kalt, B.B. Dally, Combust. Sci. Technol. 181:7 (2009) 937–953.
[28] F. Wang, J. Mi, P. Li, C. Zheng, Int. J. Hydrogen Energy 36 (2011) 9267–9277.
[29] P.R. Medwell, B.B. Dally, Combust. Flame (2012), doi: http://dx.doi.org/10.1016/j.combustflame.2012.04.012.
[30] J. Aminian, C. Galletti, S. Shahhosseini, L. Tognotti, Flow Turbul. Combust. 88 (2012) 597–623.
[31] A. Frassoldati, P. Sharma, A. Cuoci, T. Faravelli, E. Ranzi, Appl. Therm. Eng. 30 (2010) 376–383.
[32] M.M. Rahman, A. Miettinen, T. Siikonen, Numer. Heat Trans. B30 (3) (1996) 291–314.
[33] J. Warnatz, U. Mass, R.W. Dibble, Combustion, second ed., Springer, Germany, 2006 (Chapter 5).
[34] I.R. Gran, B.F. Magnussen, Combust. Sci. Technol. 119 (1) (1996) 191–217.
[35] W. Yang, D. Wei, W. Blasiak, Mathematics Modelling for High Temperature Air Combustion (HiTAC), Summary Final Report Royal Institute of Technology(KTH), 2003.
[36] A. De, E. Oldenhof, P. Sathiah, D. Roekaerts, Flow Turbul. Combust. doi: http://dx.doi.org/10.1007/s10494-011-9337-0.
[37] S.H. kim, K.Y. Hug, B.B. Dally, Proc. Combust. Inst. 30 (2005) 751–757.
[38] R. Weber, A.L. Verlaan, S. Orsino, N. Lallemant, J. Inst. Energy 72 (1999) 77.
[39] R.J. Kee, J.A. Miller, T.H. Jefferson, CHEMKIN: A General-Purpose, Problem-Independent, Transportable, Fortran Chemical Kinetics Code Package, Sandia National Laboratories, Report SAND80-8003, 1980.
[40] A. Parente, C. Galletti, L. Tognotti, Int. J. Hydrogen Energy 33 (2008) 7553–7564.
[41] A. Kazakov, M. Frenklach, Reduced Reaction Sets based on GRIMech1.2. <http://www.me.berkeley.edu/drm/>.
[42] M. Frenklach, H. Wang, C.-L. Yu, M. Goldenberg, C.T. Bowman, R. K. Hanson, et al. GRI-1.2. <http://www.me.berkeley.edu/gri_mech/>.
[43] G.P. Smith, D.M. Golden, M. Frenklach, N.W. Moriarty, B. Eiteneer, M. Goldenberg, et al. GRI-3.0. <http://www.me.berkeley.edu/gri_mech/>.
[44] P. Glarborg, R.J. Kee, J.F. Grcar, J.A. Miller, PSR: A Fortran Program for Modeling Well-Stirred Reactors; Sandia National Laboratories, Report SAND86-8209, 1986.
[45] H.J. Curran, S.M. Gallagher, J.M. Simmie, A comprehensive modelling study of methane oxidation, in: Proc. European Combustion Meeting 2003, Orleans, France.
[46] Reaction mechanisms at the Combustion Chemistry Centre, National University of Ireland, Galway. <http://c3.nuigalway.ie/mechanisms.html>.
[47] M. O'Conaire, H.J. Curran, J.M. Simmie, W.J. Pitz, C.K. Westbrook, Int. J. Chem. Kinet. 36 (2004) 603–622.
[48] S.L. Fischer, F.L. Dryer, H.J. Curran, Int. J. Chem. Kinet. 32 (2000) 713–740.
[49] H.J. Curran, P. Gaffuri, W.J. Pitz, C.K. Westbrook, Combust. Flame 114 (1998) 149–177.
[50] H.J. Curran, P. Gaffuri, W.J. Pitz, C.K. Westbrook, Combust. Flame 129 (2002) 253–280.
[51] D. Healy, H.J. Curran, J.M. Simmie, D.M. Kalitan, C.M. Zinner, A.B. Barrett, E.L. Petersen, G. Bourque, Combust. Flame 155 (2008) 441–448.
[52] D. Healy, H.J. Curran, S. Dooley, J.M. Simmie, D.M. Kalitan, E.L. Petersen, G. Bourque, Combust. Flame 155 (2008) 451–461.
[53] G. Bourque, D. Healy, H.J. Curran, C. Zinner, D. Kalitan, J. de Vries, C. Aul, E.L. Petersen, in: Ignition and Flame Speed Kinetics of Two Natural Gas Blends with High Levels of Heavier Hydrocarbons, ASME Turbo Expo 2008: Power for Land, Sea and Air, Berlin, June 9–13, 2008.
[54] P. Sabia, M. de Joannon, S. Fierro, A. Tregrossi, A. Cavaliere, Exp. Thermal Fluid Sci. 31 (2007) 469–475.